Numerical Modeling of Neutral and Charged Particles within a Gridded Ion Thruster

M. Jugroot and J.K. Harvey
Department of Aeronautics
Imperial College of Science, Technology and Medicine
SW7 2BY London
United Kingdom
m.jugroot@ic.ac.uk

IEPC-01-100

Introduction

The high specific impulse of ion thrusters and their reliability make them well suited for near-Earth and deep space missions. However, due to the complexity of transport of neutral and charged particles in the different component of these devices, the detailed properties of the ion thruster are not fully understood. Numerical simulations could be used to yield an understanding of the physical phenomena involved in thruster operation and thus help in optimizing and achieving ultra-high specific impulse ion thrusters. The external plume has been extensively studied [1,2] unlike the main chamber where many complex phenomena are suspected to occur. For this reason the present fully kinetic neutral and charged particle simulations which include the ionization processes and the applied magnetic field, investigate the processes involved at the exit of the hollow cathode and in the main chamber of an electrostatic ion thruster, T5, designed and tested [3] by the Space Department at the Defence and Evaluation Research Agency (DERA, UK). The computations presented in the paper are a continuation of those previously presented in [4] but extend these to a higher number density corresponding to levels realized in the T5 thruster.

Neutral simulation

The first part using a 3D Navier-Stokes continuum code, adapted so as to cater for the pressure differences associated with the flow, has been made previously for the neutral flow within the hollow cathode [4]. The code takes into account the heating of the insert in the hollow cathode to 1000K which is in the range of operating values. The diameter of the orifice is 0.8 mm and the gas in the hollow cathode is at an upstream pressure of 80 torr. The large pressure difference between the upstream/downstream conditions was expected to give rise to a choked flow and subsequent supersonic jet. However it was discovered that due to viscous mixing the emerging jet decelerated downstream of the cathode exit and the resulting flow was subsonic in the baffle chamber. The velocity reaches about 230 ms^{-1} (M=0.9) in the constricted area of the configuration and then decreases to around 30 ms^{-1} a few millimeters downstream.

These calculations have provided information for the upstream boundary conditions for rarified computations using particle methods for the remainder of the thruster internal flow.

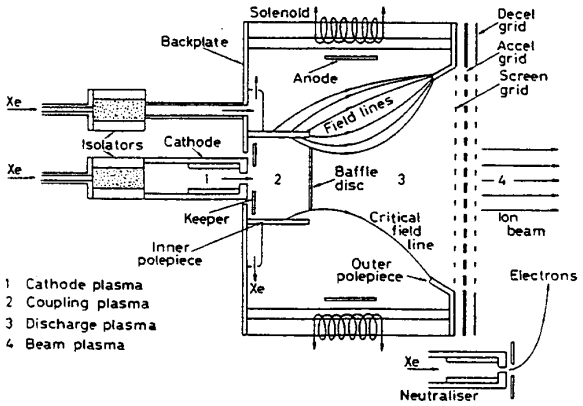

Figure 1: Schematic representation of the ion thruster.

Modeling of the post-hollow cathode regions

The post-hollow cathode regions where the pressure is observed to be several orders of magnitude lower than that in the hollow cathode is now

Presented as Paper IEPC-01-100 at the 27th International Electric Propulsion Conference, Pasadena, CA, 15-19 October, 2001.

investigated. As it is reported in the literature, a particle code is required for the discharge chamber due to the relatively low densities of particles [5]. The Direct Simulation Monte Carlo DSMC [6,7] method used in our simulations is a derivative of the well-established and numerically efficient tool for the prediction of rarefied flows.

Description of the DSMC method

The DSMC method is based on using simulator particles that mimic the behaviour of and statistically represent the very larger number of real molecules/atoms of which the fluid is comprised. Computations advance in real time but the movement of the simulators is decoupled from their collisions by modeling each of the processes alternately and independently over small, equal time increments. Candidates for inter-molecular collisions are selected from neighbouring particles in a probabilistic manner by comparing a random number with the collision probability of each pair. The outcome of each collision is determined using appropriate models, stochastic ones being the most commonly currently in use. To perform the computations, physical space is discretized into cells of the same order of magnitude as the local mean free path. The Imperial College DSMC program is a modular object-oriented code with reuse capabilities which has been adapted to take into account neutral and charged particles [8], as well as the electric field due to charge separation. The numerical Poisson solver used in this code employs a Galerkin weighed residual finite element discretization for the charges and the Langevin formulation designed for the Coulomb interactions also prevents charged particles from fleeing unrealistically the computational domain [9]. The DSMC simulation also makes use of an unstructured mesh [10] that provides great flexibility in terms of simulating geometric complexity and regions of strongly heterogeneous gradients.

DSMC modeling of the neutral flow

DSMC is therefore well adapted to the post-hollow cathode regions studied hereafter as the medium is rarefied. The first simulation describes the flow of neutral particles in the thruster and corresponds to the initiation of the discharge. The continuum code of the neutral flow provides boundary conditions at the hollow cathode exhaust for the particle modeling of the main chamber. The simulation considers the neutral particles in the ion thruster starting in a zone approximately 5 mm from the hollow cathode exit plane. The simulation has been performed with the input gas parameters from the continuum code (T = 520K; Number density = 2.46 10^{22} m^{-3}; Freestream speed ratio = 0.12). The variable soft sphere collision model [11] is employed and the collision parameters for Xenon are reference collision diameter (d=5.65Å) and viscosity temperature exponent (ω =0.85). The results show a high number density in the baffle disc region but indicates that the number density becomes diffuse and typically one order of magnitude lower outside the coupling region (see figure 1 for the schematic representation of the thruster).

Figure 2 shows the velocity of xenon particles in the thruster. The velocity is high in the aperture and forms a jet towards the exit of the thruster. The profiles indicate a recircculation zone behind the baffle disc and low velocities outside the principal flow thus implying a risk of charge exchange phenomena. The particles exit the coupling region at a relatively high speed but under the sonic threshold due to viscous mixing. The observed phenomenon at the exit of the thruster is a result of the interaction of the neutral flow and the grids (represented by a series of continuous rings) and the neutral particles exit the thruster main chamber at a subsonic speed. The results are coherent with the experimentally measured subsonic values in a Hall thruster corresponding to xenon flowing through the thruster when it is not operating [12]. The flow will accelerate beyond the sonic condition downstream on passing through the grid to leave the thruster at a very high velocity. No attempt has been made in the present study to reproduce the final acceleration process.

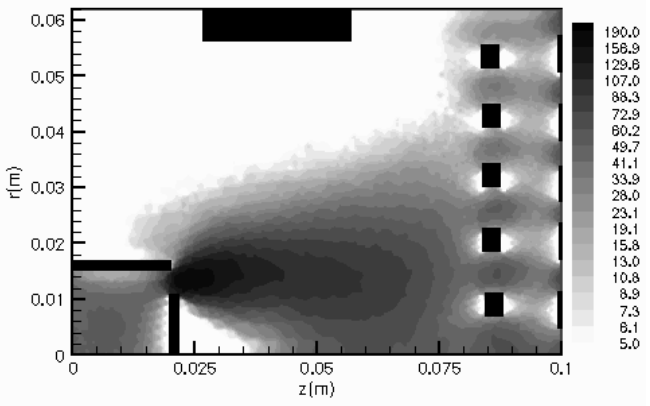

Figure 2: Velocity magnitude (m/s) of xenon.

It should be noted that both collision and plasma effects are important in the thruster. The

neutral gas is of importance and can be closely coupled to the evolution of a discharge due to the leading part it can play in ionization, joule heating, constriction etc. [13]. Traditional particle code treat only ions and electrons, i.e. there is no chemistry or electron-impact source terms – of importance in weakly ionized gases which have significant interactions between charged and neutral particles. Thus, DSMC particle simulation is also interesting from this point of view.

DSMC charged and neutral particle simulation of the main chamber

The plasma in an operating thruster can be subdivided into four closely inter-related regions depicted in figure 1. The energy of the electrons is important in defining the discharge plasma properties, since the primaries are the dominant factor controlling ionization in the discharge plasma [14]. The energy of the primaries is set by the magnitude of the voltage difference and thus the distribution of particles in the main chamber is critical information in the description of the ion thruster, characterizing performance and possible optimization.

The second part of the paper will deal with the self-consistent fully kinetic simulation of the neutral Xenon, electrons, ions and the resulting space charge in the main chamber of the ion thruster. The current axi-symmetric DSMC simulation is applied to initial conditions corresponding to electron and ion clouds (number density 10^{16} m^{-3}) [15] plus xenon neutral gas in the post-hollow cathode region (more precisely after the keeper electrode and after the potential hill, but before the baffle disc). It should be noted that previous computations [16] using a lower initial density of particles gave the same general physical results in the plasma bulk as those presented in the present paper. Due to its weak spatial extension, the sheath is not directly considered – however the effects of a sheath are taken into account at the metallic parts and the anode, by considering the absorption/repulsion of particles at the boundary conditions.

Ionization processes are known to be of paramount importance in the operation of the ion thruster. Thus, ionization is explicitly taken into consideration in the DSMC simulation at a collisional level implying no macroscopic averaging of the phenomena – this is a strong point with respect to fluid models where only global parameters can be implemented. The theory predicts that the ionization cross section will vary according to an expression in the form of

$$P = \left[1 - \frac{E_{ion}}{E}\right]^{\zeta_B} \exp\left[\frac{-\lambda E_{ion}}{E}\right]$$

[17,18], where P is the reaction probability, E is the collision energy, E_{ion} is the ionization threshold, ζ_B is a parameter related to the degrees of freedom involved in the reaction and λ is an adjustable parameter. This therefore leaves only one parameter that can be varied to fit the calculated cross sections to the measured values over the range of collision energy of interest. The cross sections measured in Xenon in [19] have been used to correlate and implement ionization in the current model.

A feature of this calculation is to relax the time restriction (due to the high mobility of electrons compared to ions) of the calculation time step by grouping electrons. This technique successfully tested in a particle simulation of the ion extraction system [20] is also applied in our previous simulations [16,21] and can be regarded to possess adequate validity to investigate the global phenomena in the main chamber. Furthermore, as the steady state (and not transient phenomena) is being investigated, the qualitative description should be reproduced.

The applied magnetic field is also implemented [21] in the simulations and differences due to its action are discussed. According to experiment, the applied magnetic field in the T5 ion thruster is principally in the direction parallel to the axis [22] and predominantly undistorted. Thus a reasonable approximation and for simplicity, only a constant longitudinal component, estimated as 25G, is represented in the computation. The effect of the magnetic field on the discharge is accounted for by the displacements it produces on the charged particles. These are defined by the Lorentz equation and are integrated over every time increment in the simulation. In fact, only a small fraction of the circular-like orbits due to the action of the electric and magnetic field are realized during the individual time-steps, as the trajectories are interrupted by collisions.

A screen grid and an accelerating grid have been implemented at the exit plane of the thruster, since they will have a significant influence on the flow of charged particles due to the voltage applied and neutral particles due to the porosity. In this axi-symmetric representation, the screen grid is simplified and modeled by a series of continuous rings representing the holes of the grid. All the numerous

holes are not represented so as conserve a reasonable cell count in the simulation while retaining the same open area ratio (open.area/closed.area ~ 60%). Similarly the screen-to-accelerating grid distance has been overestimated for the same reasons but same ratios between different parameters are adopted. The voltage applied to the screen grid is 1100V and that of the accelerating grid is of –250V.

The current simulations aim at capturing the physical phenomenology involved within the main chamber via the population of the charged particles.

Results and discussion

Figures 3 and 4 represent the electron number density in the main chamber (without and with the applied magnetic field respectively). Globally it can be observed that the electron density is diffuse in the main body of the chamber in both cases. However, it can clearly be noted that the density of electrons drops severely in the screen grid region. The depletion of electrons is a direct consequence of the potential distribution at the exit grid system. The calculations indicate that a negative potential builds up from the accelerating grid and extends a few millimeters towards the screen grid. It is known that one of the aims of the screen grid is to repel the electrons and prevent them from leaving the main chamber [20,23], achieved by the plasma sheath formed near the grid. Thus, the potential distribution of the sheath and the resulting effects are qualitatively reproduced by our steady state calculations as the electrons are repelled from the exit zone and constrained within the main chamber. The distribution and the magnitude of the potential and the resulting electric field at the grids and the resulting electric field therefore imply that effective only ions can exit through the exit grid apertures. The ion number density between the screen grids depicted in figure 6 proves that ions are leaving the main chamber.

Overall, we observe that the ion density is diffused throughout the chamber in both cases. The medium is globally quasi-neutral in the bulk of the main chamber (except near the walls due to unequal absorption/repulsion of particles; and beyond the screen grid as only ions exit the grid), as depicted on figure 5. Variations in the quoted contour values of the ratio of the number density of ions to electrons occur partly due to the numerical scatter in the DSMC method. However, a spatial repartition exists between the two charged species and a net charge exists in certain localized regions of the main chamber.

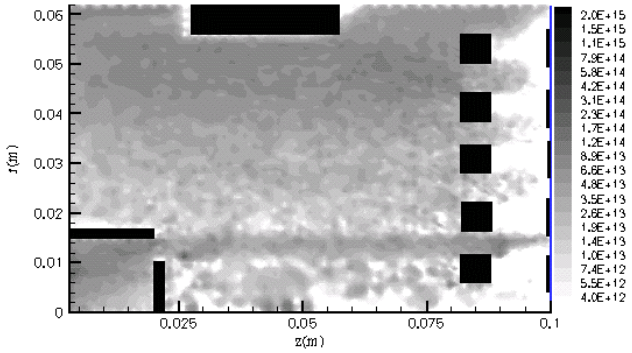

Figure 3: Number density of electrons in the main chamber of ion thruster (no magnetic field applied).

The electron density is highest in the outer central zone of the main chamber (in both cases) where ionization is more important as a result of space charge. In fact, the number density of ions is high in the anode region, and thus the positive net charge generated in that region in turn induces a higher electric field and thus an enhanced ionization leads to an accumulation of electrons in the outer central zone of the main chamber. This is more apparent when the magnetic field is applied (figure 4) which enhances ionization due to the increase in the path of electrons by allowing them to encounter more ionization collisions. Hence the number density of electrons is somewhat higher in the central upper position as depicted in figure 4 compared to figure 3. The applied magnetic field case clearly illustrates that more electrons are present in the main chamber. Due to the axi-symmetrical configuration, the higher electron densities situated in the outer regions imply that a significantly larger number of electrons are produced and constrained inside the main chamber.

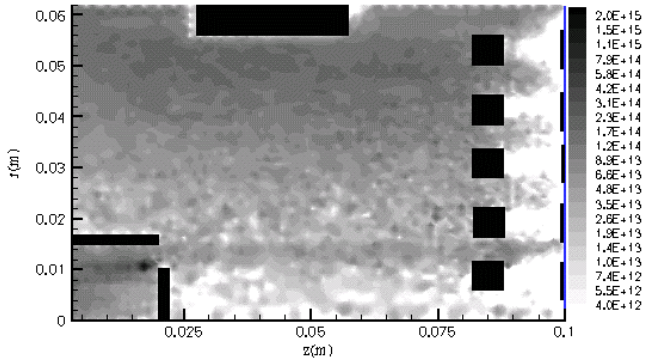

Figure 4: Number density of electrons in the main chamber of ion thruster (with magnetic field applied).

The number density of electrons exceeds that of ions in the axial region beyond the baffle disc as a consequence of the transverse electric field. In fact, as a result of the different mobilities of electrons and ions, a space-charge-induced transverse electric field is created. The transverse electric field has a localized range but plays an important part in the distribution of the electrons. Hence, the transverse electric field near the axial region creates a focusing effect and retains the electrons towards the axial region. This effect is perceptible on electrons, whereas ions are unaffected due to their larger mass. Due to the new spatial distribution of space charge when the magnetic field is applied, the transverse electric field is comparatively higher and thus relatively more efficient in focusing the electrons towards the axial zone.

The aperture of the baffle disc is another region where the space-charge-generated electric field is important. The distribution of the space charge and the related electric field probably play an important role in the transition of particles from the coupling zone to the discharge zone. In fact, the space charge is first positive in the coupling plasma and then negative near the baffle disc and then positive again in the discharge plasma region. This implies that an electron flowing through the aperture experiences drastic changes in the magnitude of forces while crossing this critical zone, where complex behaviours have experimentally been detected [14]. It should be noted that the action of the magnetic field on the distribution on species also modifies the net charge in that region.

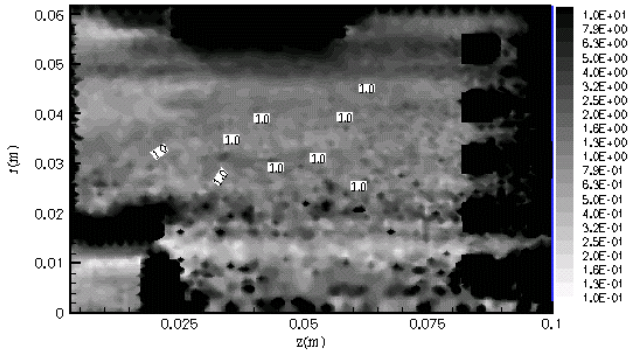

Figure 5: Ratio of number density of ions to that of electrons in the main chamber, n_i/n_e (with magnetic field applied).

Globally, the applied magnetic field can have a direct repercussion on the net charge because of the change brought about in the particles' trajectories. The magnetic field increases the path of electrons leading to an increase of ionization processes. This induces a change of particle distribution and the related space charge, directly related to the electric field and velocity of the charged particles. Thus the change in velocity of the charged species in turn changes the path of the particles and the whole process describes the close coupling of these effects. This intricate relationship has a localized range but can play a governing role in certain regions of the discharge. The action of the magnetic field on the distribution of particle is even more apparent when the electric field/net charge is high, i.e. in zones where ionization is important.

There are also significantly more ions in the main chamber in the applied magnetic field case as shown in figure 6. Locally the ion number density is higher in the anode region due to enhanced ionization compared to the case where the applied magnetic field is absent. The ion number density is also lower in the axial region past the baffle disk region but that zone remains dominated by electrons, which are more numerous due to the focusing action of the transverse electric field. The magnetic field indirectly promotes a more uniform drift of ions towards the extraction grids by the modification of the electric field due to the change in the space charge/particle distribution.

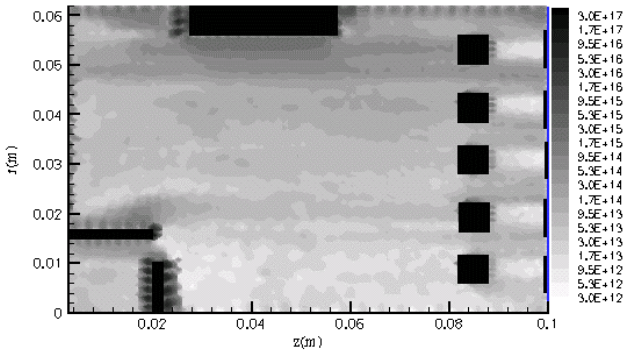

Figure 6: Number density of ions in the main chamber of ion thruster (with magnetic field applied).

Qualitative insights can be obtained by examining the figures showing the distribution of particles within the main chamber. A more refined applied magnetic field mapping, for instance, for the baffle disc region, would allow closer investigation of the coupling region where several complex regimes are reported to occur [24]. A further step in our work will be to use the densities obtained near the screen grid in this study as the stating point for a DSMC simulation of a single set of grid apertures so as to gain

a more detailed understanding of the competing physical phenomena inherent to the ion thruster device.

Conclusion

The continuum code has helped in developing an understanding of the flow in the hollow cathode nozzle and has shown the localized high velocity and the sharp drop in pressure after the nozzle, implying the importance of using a particle model in the post-hollow cathode region. DSMC calculations have therefore been performed for neutral particles (with input parameters from the continuum code) for the post-hollow cathode region. Calculations have also been performed for the charged and neutral particles in the main chamber, with ionization processes being explicitly taken into account in the particle code. These simulations provide a qualitative description of the details of the flow of particles within the main chamber. The charged particles are globally diffuse in the main chamber in spite of ionization, but net charge related effects and enhanced ionization in certain localized regions both play a leading role. The addition of the magnetic field indicates that presumably ionization is enhanced due to the increase in the path of electrons and that the coupled action with net charge participates fully in the distribution of charged particles in the main chamber.

Acknowledgements

This work is supported by the EPSRC Grant GL/L42964 "Engineering Optimisation of Kaufman-type electrostatic ion thrusters for space missions". The authors wish to thank Prof. M.G. Haines, Dr. A.K. Malik, Mr. S.W. Patterson (Imperial College) and Dr. D.G. Fearn (DERA) for very helpful discussions.

References

[1] R.I. Samanta Roy, D.E. Hastings, S. Taylor, *Journal of Computational Physics*, 126, 1996

[2] D.B. Van Gilder, G.I. Font, I.D. Boyd, *Journal of Propulsion and Power*, 15, 4, 1999

[3] N.C Wallace, D.H. Mundy, D.G. Fearn, C.H. Edwards, *35th Joint Propulsion Conference and Exhibit*, AIAA Paper 99-2442, Los Angeles, California, 1999

[4] M. Jugroot, J.K. Harvey, *The Aeronautical Journal*, 105, 2001

S.W. Patterson, M. Jugroot, D.G. Fearn, *36th Joint Propulsion Conference and Exhibit*, AIAA Paper 2000-3532, Huntsville, Alabama, 2000

[5] X. Peng, D. Keefer, W.M. Ruyten, *Journal of Propulsion and Power*, 8, 2, 1992

[6] G.A. Bird, *Molecular Gas Dynamics and the direct simulation of gas flows*, Clarendon Press, 1994

[7] E.S. Oran, C.K. Oh, B.Z. Cybyk, *Annual Review of Fluid Mechanics*, 30, 1998

[8] M.A. Gallis J.K. Harvey, *21st International Symposium on Rarefied Gas Dynamics*, Marseille, France, 1998

T.L. Parsons, M.A. Gallis, J.K. Harvey, *21st International Symposium on Rarefied Gas Dynamics*, Marseille, France, 1998

[9] M.A. Gallis, R. Prasad, J.K. Harvey, *29th AIAA Plasmadynamics and Lasers Conference*, AIAA Paper 98-2666, Albuquerque, NM, 1998

[10] Gambit, Fluent Inc., 1998

[11] K. Koura, H. Matsumoto, *Physics of Fluids A*, 4, 1992

[12] R.J. Cedolin, W.A. Hargus, P.V. Storm, R.K. Hanson, M.A. Cappelli, *Applied Physics B*, 65, 1997

[13] M. Jugroot, P. Bayle, M. Yousfi, O. Eichwald, *Journal of Physics D: Applied Physics*, 32, 1999

[14] D.J. Milligan, S.B. Gabriel, *26th International Electric Propulsion Conference*, Paper IEPC 99-157, Kitakyushu, Japan, 1999

[15] J.D. Williams, P.J. Wilbur, *Journal of Spacecraft and Rockets*, 29, 6, 1992

I. Kameyama, P. Wilbur, *21st International Symposium on Space Technology and Science*, ISTS 98-a-2-17, Japan, 1998

[16] M. Jugroot, J.K. Harvey, *Proceedings of the 10th International Congress on Plasma Physics*, Quebec, Canada, 2000

[17] M.A. Gallis, J.K. Harvey, *31st AIAA Thermophysics Conference*, AIAA Paper 96-1849, New Orleans, LA, 1996

[18] M.A. Gallis, J.K. Harvey, *Physics of Fluids*, 10(6), 1998

M.A. Gallis, J.K. Harvey, *J. Fluid Mech*., 312, 1996

[19] D. Rapp, G.P. Englander, *Journal of Chemical Physics*, 43, 1965

[20] Y. Okawa, H. Takegahara, *26th International Electric Propulsion Conference*, Paper IEPC-99-146, Kitakyushu, Japan, 1999

[21] M. Jugroot, J.K Harvey, *Proceedings of the 3rd International Conference on Spacecraft Propulsion*, ESA SP-465, Cannes, France, 2000

[22] S.N. Moore, *25th International Electric Propulsion Conference*, IEPC Paper 97-017, Cleveland, Ohio, 1997

[23] G. Aston, P.J. Wilbur, *Journal of Applied Physics*, 52(4), 1981

[24] A. K. Malik, *26th International Electric Propulsion Conference*, IEPC Paper 99-141, Kitakyushu, Japan, 1999